nature climate change

LETTERS

PUBLISHED ONLINE: 9 FEBRUARY 2015 | DOI: 10.1038/NCLIMATE2524

Attribution of Arctic temperature change to greenhouse-gas and aerosol influences

Mohammad Reza Najafi[1]*, Francis W. Zwiers[1] and Nathan P. Gillett[2]

The Arctic has warmed significantly more than global mean surface air temperature over recent decades[1], as expected from amplification mechanisms[2,3]. Previous studies have attributed the observed Arctic warming to the combined effect of greenhouse gases and other anthropogenic influences[4]. However, given the sensitivity of the Arctic to external forcing and the intense interest in the effects of aerosols on its climate[5,6], it is important to examine and quantify the effects of individual groups of anthropogenic forcing agents. Here we quantify the separate contributions to observed Arctic land temperature change from greenhouse gases, other anthropogenic forcing agents (which are dominated by aerosols) and natural forcing agents. We show that although increases in greenhouse-gas concentrations have driven the observed warming over the past century, approximately 60% of the greenhouse-gas-induced warming has been offset by the combined response to other anthropogenic forcings, which is substantially greater than the fraction of global greenhouse-gas-induced warming that has been offset by these forcings[7,8]. The climate models considered on average simulate the amplitude of response to anthropogenic forcings well, increasing confidence in their projections of profound future Arctic climate change.

We analyse observed near-surface air temperature anomalies over land from the circumpolar region north of 65° N using gridded temperature observations from the CRUTEM4 (Climatic Research Unit gridded land temperature data, version 4) data set. Although spatial coverage over the Arctic remains limited by the availability of long-term station data, coverage is considerably improved compared with a previous version of the data set[9]. This data set consists of gridded (5° × 5°) monthly mean surface temperature anomalies that are expressed relative to the 1961–1990 climatology. To focus on long-term changes we calculate non-overlapping five-year seasonal and annual means for five-year periods beginning with 1913–1917 and ending with 2008–2012. Five-year means are calculated only when more than 50% of potentially available data are present over each period, and are otherwise flagged as missing. Grid cells for which 70% of five-year means can be calculated are included in the analysis.

We compare observed Arctic temperature anomalies with output from nine CMIP5 (Fifth Phase of the Coupled Model Intercomparison Project) climate models that provide climate simulations to 2012 with historical greenhouse-gas changes (GHG), historical natural forcing (NAT), and historical variations in all forcing agents combined (ALL), including greenhouse gases, aerosol, ozone, land cover and natural forcings. Note that overall, CMIP5 models have improved simulations of Arctic sea-ice changes compared with earlier generation models[10]. A total of 35 forced simulations were available for each forcing combination from the nine models combined (bcc-csm1-1, CanESM2, CNRM-CM5, CSIRO-Mk3-6-0, GISS-E2-H, GISS-E2-R, HadGEM2-ES, IPSL-CM5A-LR and NorESM1-M) as detailed in Supplementary Table 1. Most CMIP5 historical ALL simulations end in 2005, and thus we use either extended ALL simulations provided by some modelling centres or simulations extended from 2005 to 2012 with the corresponding RCP4.5 (Representative Concentration Pathway emissions scenario with approximate total radiative forcing in year 2100 relative to 1750 of 4.5 W m^{-2}) simulations. In addition, we use 24,800 years of pre-industrial control simulation from 42 CMIP5 models (Supplementary Table 2) to assess internal climate variability.

Model output is processed to replicate the availability of the observations as closely as possible. CMIP5 near-surface air temperatures over land are re-gridded to the spatial resolution of CRUTEM4 (5° × 5°), and each simulation is masked by the observational coverage to ensure consistent spatial and temporal coverage with observations. We remove the seasonal cycle by subtracting the 1961–1990 climatology for individual months to produce monthly anomalies, and calculate non-overlapping five-year means as for the observations, using the same criteria for data availability.

Observations and historical simulations with ALL forcing agents show warming throughout the Arctic land regions (Fig. 1), with greater warming in Siberia, Alaska and Canada. The multi-model GHG forcing response, which does not include the cooling effect of anthropogenic aerosol emissions, shows a stronger warming trend than observed. The multi-model response to the other anthropogenic forcings consisting of aerosols, ozone and land use change (OANT), which is estimated by subtracting the responses to GHG and NAT forcings from ALL, exhibits a consistent cooling effect for all regions. Previous modelling results have demonstrated that the cooling effect of aerosols on Arctic climate is much larger than the small warming due to ozone changes, with land use change having a negligible effect[11]; hence, OANT is dominated by aerosol changes. Note that NorESM1-M includes time-varying ozone in its single GHG simulation in contrast to all other models that include only the well-mixed greenhouse gases in their GHG simulations.

Observed Arctic mean temperature shows a warming trend in the first part of the century, followed by a cooling from the 1940s to the 1970s, and subsequently a strong warming trend in the most recent decades (Fig. 2). Previous studies have suggested that both internal variability and anthropogenic forcing[11] may have contributed to the warming trend in the 1930s and 1940s, and that the cooling between the 1940s and 1970s may have been caused largely by anthropogenic aerosols and natural forcing[12]. The ALL simulations closely follow the evolution of observed temperatures from 1952 to 2012, but they underestimate the warming during the early

[1]Pacific Climate Impacts Consortium, University House 1, University of Victoria, PO Box 1700 STN CSC, Victoria, British Columbia V8W 2Y2, Canada.
[2]Canadian Centre for Climate Modelling and Analysis, Environment Canada, PO Box 1700 STN CSC, Victoria, British Columbia V8W 2Y2, Canada.
*e-mail: rnajafi@uvic.ca

© 2015 Macmillan Publishers Limited. All rights reserved.

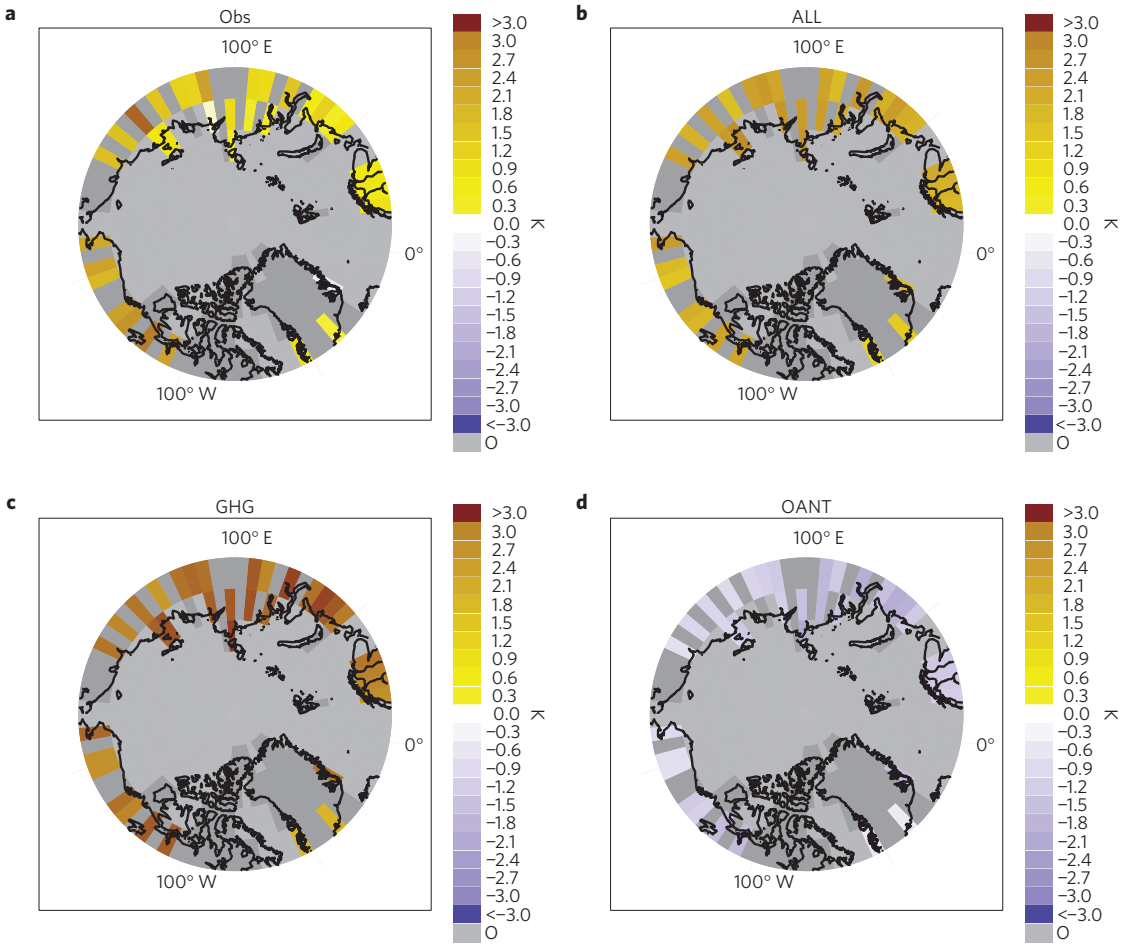

Figure 1 | Simulated and observed 1913–2012 temperature trends over the Arctic. a–d, CRUTEM4 observations (**a**), and CMIP5 multi-model ensemble averages based on 9 models and 35 ensemble members for each type of forcing: ALL (**b**), GHG (**c**) and OANT (**d**). Land areas with no data are shaded dark grey and ocean areas are shaded the lighter grey indicated by 'O' on the colour scale. Trends are calculated from 5-yr means. ALL corresponds to simulations with all major anthropogenic and natural forcings, GHG corresponds to simulations forced by greenhouse-gas changes, and OANT corresponds to simulations forced by anthropogenic forcings other than greenhouse gases.

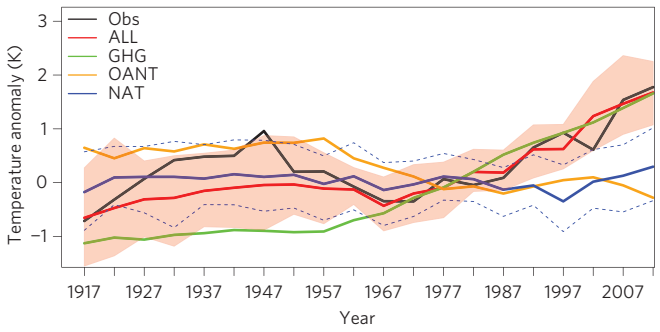

Figure 2 | Simulated and observed Arctic temperature anomalies. Observed 5-yr mean Arctic mean temperature anomalies (black) are compared with the mean simulated response to all anthropogenic and natural forcings (red), greenhouse-gas changes (green), other anthropogenic forcings (orange) and natural forcings (blue). Red shading and blue dashed lines represent the 5–95% uncertainty ranges corresponding to ALL and NAT responses respectively.

twentieth century. The observed Arctic mean temperature generally falls within the 90% range of the individual ALL simulations. As expected, the ensemble mean of the GHG simulations warms monotonically from the late 1950s onwards. In contrast, the NAT simulations show interannual variability with no significant long-term trends. The estimated response to OANT forcing exhibits cooling from the late 1950s to the late 1970s, reflecting changes in aerosol forcing during this period[13], but shows little change during recent decades.

We quantify the separate contributions from greenhouse gases (GHG), other anthropogenic forcing agents (OANT), and natural forcings (NAT) to observed Arctic temperature change using an optimal fingerprinting approach[14]. This entails regressing observed temperature anomalies onto model-simulated ensemble mean responses to GHG, OANT and NAT forcing using a total least-squares algorithm. The resulting scaling factors, which scale the simulated responses to best reproduce the observed changes, and their 90% confidence intervals are shown in Fig. 3a for both the multi-model ensemble mean responses and the individual-model ensemble mean responses. A positive scaling factor that is inconsistent with zero implies that the signal is detected at the 5% significance level. Scaling factors close to unity with small uncertainty ranges imply good agreement between observed and model-simulated changes. The multi-model GHG and OANT responses are both robustly detected, with a GHG scaling factor very close to one, and an OANT scaling factor above one, suggesting some under-estimation of the OANT response in the multi-model mean. Most individual-model GHG and OANT signals are also detected. In contrast, the multi-model response to natural forcing

© 2015 Macmillan Publishers Limited. All rights reserved.

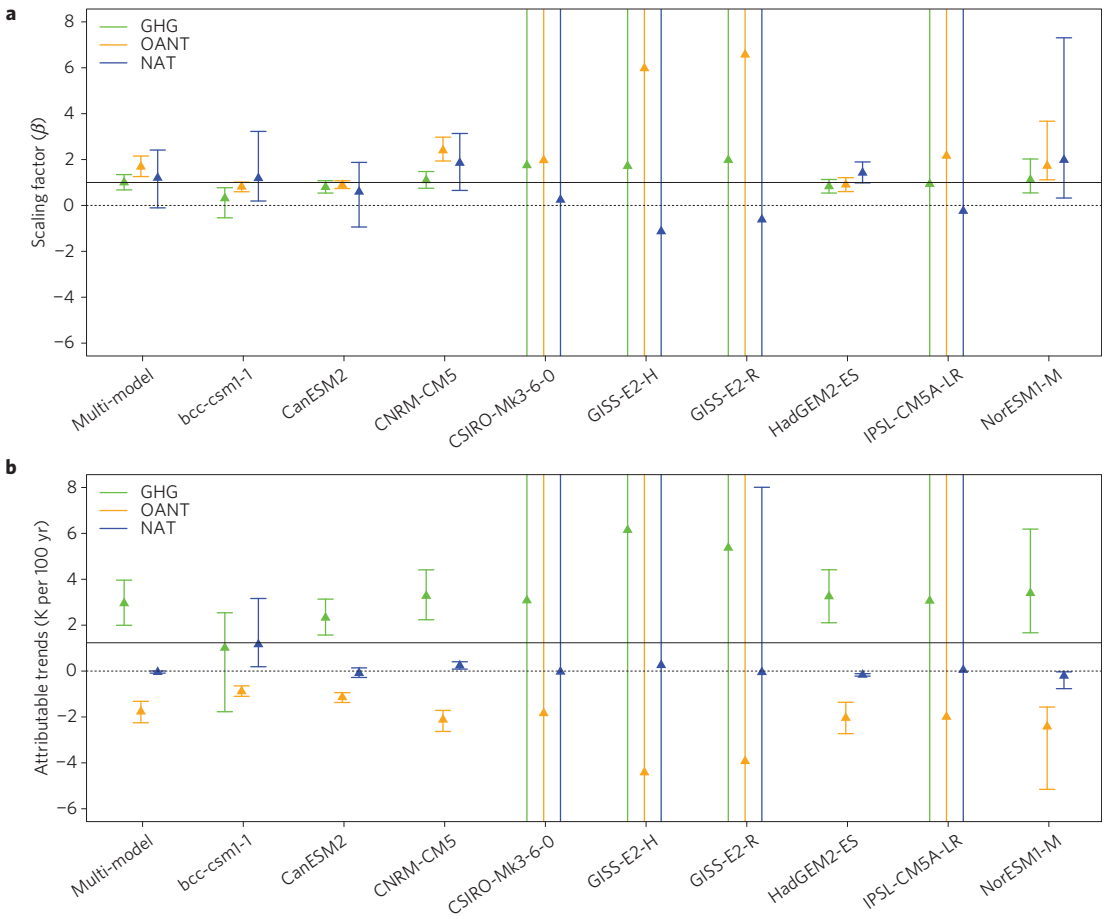

Figure 3 | Scaling factors by which the simulated Arctic temperature response to GHG, OANT and NAT should be multiplied to best match observations and corresponding attributable temperature trends. a, Scaling factors are derived from regressions of observed 5-yr Arctic mean temperature anomalies over the 1913–2012 period onto the simulated responses to GHG, OANT and NAT forcings, from individual CMIP5 models and the multi-model mean; 5–95% confidence intervals are shown by bars and corresponding best estimates are represented by triangles. Scaling factors inconsistent with zero indicate a detectable response to the forcing concerned. **b**, Corresponding attributable temperature trends (in K per 100 yr). The solid horizontal line indicates the observed Arctic-average temperature trend.

is not robustly detected, although it is detected using four of the models individually. The estimates of the responses to external forcing from single models are more uncertain than multi-model response estimates owing to smaller ensemble sizes, which mean that single-model response estimates are more strongly affected by internal variability, as well as model uncertainty[7]. The residual consistency test[15] is passed in all but two cases (CNRM-CM5 and GISS-E2-H), indicating that the residual variability that remains in the observations after removing the scaled responses is consistent with internal variability in the region as simulated in the climate model control simulations. To assess the sensitivity of the results to spatial coverage we also performed the analysis for the region poleward of 60° N (Supplementary Fig. 1), obtaining consistent results (Supplementary Fig. 2). Changing the criterion for the inclusion of grid boxes from a minimum 50% land fraction to at least 95% land fraction, which removes most coastal grid boxes that extend over water-covered areas, had negligible impact on GHG and OANT detection.

Warming trends over 1913–2012 attributable to GHG, OANT and NAT are obtained by multiplying the trends in the multi-model forced responses by the estimated scaling factors (Fig. 3b). On the basis of the multi-model responses, it is estimated that GHGs alone would have warmed the Arctic by 3 °C [2–4 °C] over the past century, and that this has been offset by 1.8 °C [1.3–2.2 °C] of cooling induced by OANT forcing, to produce a net warming effect that is very close to the observed warming of 1.2 °C. Natural forcing (NAT) has not contributed to the observed long-term warming in a discernible way. To assess the robustness of our findings, we conducted a similar analysis for individual seasons as shown in Supplementary Fig. 3. The individual responses to greenhouse gases and other anthropogenic forcings are detected in all seasons. On the basis of the best estimates of attributed temperature changes, OANT forcing is estimated to have offset approximately 60% of the estimated GHG-induced warming in the Arctic over the period 1913–2012. This is substantially greater than on the global scale, for which one set of estimates of attributable GHG, OANT and NAT trends suggests that about 5% of the GHG-induced warming over the period 1901–2010 (and about 27% for 1951–2010) may have been offset by cooling from OANT (ref. 8).

To further evaluate the robustness of our findings, we repeat our analysis with two additional observational data sets: the Goddard Institute for Space Studies (GISS) surface temperature data set[12] (Supplementary Fig. 4), and Merged Land–Ocean Surface Temperature analysis (MLOST) data set provided by the NOAA/OAR/ESRL PSD, Boulder, Colorado, USA, from their website at http://www.esrl.noaa.gov/psd (ref. 16; Supplementary Fig. 5). These data sets were also assessed in the Intergovernmental Panel on Climate Change (IPCC) Fifth Assessment Report[17]. Unlike CRUTEM4, GISS and MLOST employ infilling techniques for some locations with no station data and to estimate surface air

© 2015 Macmillan Publishers Limited. All rights reserved.

temperature anomalies over some ocean areas, although little sea surface temperature data exist over the Arctic. As shown in Supplementary Fig. 6, results obtained using the GISS and MLOST data sets, with their greater Arctic coverage, are very consistent with those obtained with the CRUTEM4 data set.

Our results demonstrate that both greenhouse-gas changes and changes in aerosols and other anthropogenic forcings have made significant contributions to observed interdecadal variations in Arctic land temperature over the past century. Although a role for aerosols in driving mid-century Arctic cooling has previously been proposed on the basis of analysis of model simulations[11], these results demonstrate for the first time that an aerosol contribution to multi-decadal temperature variations is detectable in observations. Moreover, our results demonstrate that aerosol-induced cooling has offset between 1.3 and 2.2 °C of greenhouse-gas-induced warming over the past century, and thus that without it the large observed Arctic warming of 1.2 °C would have been even larger. This offset seems to have been relatively more important in the Arctic than in the global mean. Significant climate impacts of Arctic warming are already occurring such as permafrost warming[18], reductions in sea-ice extent[19,20], and changes in glacier and ice-sheet mass balance[21]. Over the coming decades, aerosol emissions are projected to decrease[22], with greenhouse gases increasing strongly, implying that the rate of Arctic warming is likely to increase. Our results demonstrate that the CMIP5 models considered on average simulate the response to greenhouse gas realistically and slightly underestimate the response to aerosol changes over the Arctic. The CMIP5 models simulate a mean Arctic warming of 8.3 °C by the end of the century under the business-as-usual RCP8.5 scenario[23]. By demonstrating the broad consistency of simulated and observed responses to greenhouse gases and other anthropogenic forcings, our results provide confirmation that the profound future Arctic climate change projected by climate models under such scenarios is likely to be realized unless greenhouse-gas emissions are strongly reduced.

Methods

We used a total least-squares optimal fingerprinting approach[14,24] for detection and attribution, which uses a generalized linear regression model to represent observed changes as a linear combination of GHG-, OANT- and NAT-induced changes. The regression model represents observations as

$$T_{obs} = \beta_1 T_{ALL} + \beta_2 T_{NAT} + \beta_3 T_{GHG} + \varepsilon$$

where T_{obs} is a vector of observed temperature anomalies, T_{ALL}, T_{NAT} and T_{GHG} are estimates of the responses to ALL, NAT and GHG forcing respectively, the β terms are corresponding scaling factors and ε is residual variability that is generated internally in the climate system. Scaling factors for T_{GHG}, T_{OANT} *and* T_{NAT} are obtained by decomposing T_{ALL} as $T_{ALL} = T_{GHG} + T_{NAT} + T_{OANT}$ and substituting as follows:

$$T_{obs} = (\beta_1 + \beta_3) T_{GHG} + (\beta_1 + \beta_2) T_{NAT} + \beta_1 T_{OANT} + \varepsilon$$

$$\beta_{GHG} = \beta_1 + \beta_3, \beta_{NAT} = \beta_1 + \beta_2, \beta_{OANT} = \beta_1$$

Fitting the regression model requires estimates of the covariance structure of internal climate variability, which are constructed using unforced control simulations. The regression model is fitted without resorting to an empirical orthogonal function truncation to reduce the dimension of the detection space because sufficient control simulations are available to estimate full-rank covariance matrices. A residual consistency test is used to compare model-simulated internal variability with observations.

Received 8 August 2014; accepted 4 January 2015; published online 9 February 2015

References

1. Christensen, J. H. *et al.* in *Climate Change 2013: The Physical Science Basis* (eds Stocker, T. F. *et al.*) Ch. 14 (IPCC, Cambridge Univ. Press, 2013).
2. Cohen, J. L., Furtado, J. C., Barlow, M. A., Alexeev, V. A. & Cherry, J. E. Arctic warming, increasing snow cover and widespread boreal winter cooling. *Environ. Res. Lett.* **7,** 014007 (2012).
3. Screen, J. A. & Simmonds, I. The central role of diminishing sea ice in recent Arctic temperature amplification. *Nature* **464,** 1334–1337 (2010).
4. Gillett, N. P. *et al.* Attribution of polar warming to human influence. *Nature Geosci.* **1,** 750–754 (2008).
5. Arctic Council Task Force on Short-Lived Climate Forcers *Recommendations to Reduce Black Carbon and Methane Emissions to Slow Arctic Climate Change* (Arctic Council, 2013).
6. Shindell, D. Estimating the potential for twenty-first century sudden climate change. *Phil. Trans. R. Soc. A* **365,** 2675–2694 (2007).
7. Bindoff, N. L. *et al.* in *Climate Change 2013: The Physical Science Basis* (eds Stocker, T. F. *et al.*) Ch. 10 (IPCC, Cambridge Univ. Press, 2013).
8. Jones, G. S., Stott, P. A. & Christidis, N. Attribution of observed historical near-surface temperature variations to anthropogenic and natural causes using CMIP5 simulations. *J. Geophys. Res. Atmos.* **118,** 4001–4024 (2013).
9. Jones, P. *et al.* Hemispheric and large-scale land-surface air temperature variations: An extensive revision and an update to 2010. *J. Geophys. Res.* **117,** D05127 (2012).
10. Flato, G. *et al.* in *Climate Change 2013: The Physical Science Basis* (eds Stocker, T. F. *et al.*) Ch. 9 (IPCC, Cambridge Univ. Press, 2013).
11. Fyfe, J. C. *et al.* One hundred years of Arctic surface temperature variation due to anthropogenic influence. *Sci. Rep.* **3,** 2645 (2013).
12. Hansen, J., Ruedy, R., Sato, M. & Lo, K. Global surface temperature change. *Rev. Geophys.* **48,** RG4004 (2010).
13. Myhre, G. *et al.* in *Climate Change 2013: The Physical Science Basis* (eds Stocker, T. F. *et al.*) Ch. 8 (IPCC, Cambridge Univ. Press, 2013).
14. Allen, M. & Stott, P. Estimating signal amplitudes in optimal fingerprinting, Part I: Theory. *Clim. Dynam.* **21,** 477–491 (2003).
15. Ribes, A., Planton, S. & Terray, L. Application of regularised optimal fingerprinting to attribution. Part I: Method, properties and idealised analysis. *Clim. Dynam.* **41,** 2817–2836 (2013).
16. Smith, T. M., Reynolds, R. W., Peterson, T. C. & Lawrimore, J. Improvements to NOAA's historical merged land–ocean surface temperature analysis (1880–2006). *J. Clim.* **21,** 2283–2296 (2008).
17. Hartmann, D. L. *et al.* in *Climate Change 2013: The Physical Science Basis* (eds Stocker, T. F. *et al.*) Ch. 2 (IPCC, Cambridge Univ. Press, 2013).
18. Stieglitz, M., Déry, S., Romanovsky, V. & Osterkamp, T. The role of snow cover in the warming of arctic permafrost. *Geophys. Res. Lett.* **30,** 1721 (2003).
19. Kay, J. E., Holland, M. M. & Jahn, A. Inter-annual to multi-decadal Arctic sea ice extent trends in a warming world. *Geophys. Res. Lett.* **38,** L15708 (2011).
20. Parkinson, C. L. & Comiso, J. C. On the 2012 record low Arctic sea ice cover: Combined impact of preconditioning and an August storm. *Geophys. Res. Lett.* **40,** 1356–1361 (2013).
21. Shepherd, A. *et al.* A reconciled estimate of ice-sheet mass balance. *Science* **338,** 1183–1189 (2012).
22. Gillett, N. P. & Von Salzen, K. The role of reduced aerosol precursor emissions in driving near-term warming. *Environ. Res. Lett.* **8,** 034008 (2013).
23. Collins, M. *et al.* in *Climate Change 2013: The Physical Science Basis* (eds Stocker, T. F. *et al.*) Ch. 12 (Cambridge Univ. Press, 2013).
24. Hasselmann, K. Multi-pattern fingerprint method for detection and attribution of climate change. *Clim. Dynam.* **13,** 601–611 (1997).

Acknowledgements

We acknowledge the Program for Climate Model Diagnosis and Intercomparison and the World Climate Research Programme's Working Group on Coupled Modelling for their roles in making the WCRP CMIP5 multi-model data sets available. This work is supported by the NSERC Canadian Sea Ice and Snow Evolution (CanSISE) Network.

Author contributions

M.R.N., F.W.Z. and N.P.G. designed analysis. M.R.N. conducted the analysis and wrote the initial draft. F.W.Z. and N.P.G. helped with the analysis and edited the manuscript.

Additional information

Supplementary information is available in the online version of the paper. Reprints and permissions information is available online at www.nature.com/reprints. Correspondence and requests for materials should be addressed to M.R.N.

Competing financial interests

The authors declare no competing financial interests.

© 2015 Macmillan Publishers Limited. All rights reserved.